Research Article

Parameterized Deceleration in f(Q, C) Gravity: A Logarithmic Approach

S. R. Bhoyar[1], Yash Ingole[1]

1. Department of Mathematics, Phulsing Naik Mahavidyalaya, India

This study explores a novel logarithmic parameterization of the deceleration parameter within the $f(Q,C)$ gravity framework, incorporating a nonlinear functional form $f(Q,C) = \gamma_1 Q^n + \gamma_2 C$, where Q and C denote the nonmetricity scalar and boundary term, respectively, and $n \geq 1$. This approach provides a distinctive perspective on the universe's accelerated expansion without resorting to exotic fields. Using observational data from Hubble measurements (OHD) and the $Pantheon + SH0ES$ Type Ia supernovae dataset, the model parameters were constrained through a χ^2 minimization technique. The analysis reveals a transition from deceleration to acceleration in the universe's expansion history, with the transition redshifts $z_t \approx 0.98$ (OHD) and $z_t \approx 0.76$ ($Pantheon + SH0ES$). The model demonstrates consistency with observations, offering insights into the dynamics of dark energy and alternative gravity theories, while effectively modeling cosmic evolution across epochs.

I. Introduction

Recent observations have significantly altered our understanding of the universe, revealing that its expansion is currently accelerating[1][2]. Evidence from various sources, including Type Ia Supernovae (SNeIa), Cosmic Microwave Background (CMB) radiation, and Baryon Acoustic Oscillations (BAO)[3][4], has consistently indicated this acceleration, implying the presence of an energy form with significant negative pressure, commonly known as dark energy (DE), which contributes nearly 70% to the current energy budget of the universe. Several DE models have been proposed to explain this phenomenon. The cosmological constant (Λ), which corresponds to a simple equation of state with ($\omega = -1$), indicates a constant energy density across space and time, which being the simplest and most widely accepted. However, the ΛCDM model faces critical challenges, such as the fine-tuning problem[5], the coincidence problem[6], and the age problem[7], which call for alternative explanations for the nature and origin of DE. In response to these issues, scalar field models both canonical and noncanonical have gained prominence as they provide a more dynamic and versatile framework for describing cosmic evolution. Over the past decade, numerous DE models, including quintessence, K-essence, phantom energy, tachyon fields, and Chaplygin gas, have been explored as potential candidates for explaining cosmic acceleration (see ref.[8] for a comprehensive review). Despite this progress, a universally accepted and definitive DE model remains elusive.

These unresolved issues have encouraged the exploration of modified gravity theories, which aim to provide alternative explanations for the universe's accelerated expansion. Rather than relying on exotic energy components such as DE, these theories propose that cosmic acceleration could arise from modifications to the fundamental laws of gravity. In the following passage, we delve into the various modified gravity models, focusing on how they extend the standard framework of General Relativity (GR) and offer new insights into the dynamics of the cosmos.

Modified theories of gravity are advanced frameworks designed to extend or refine the GR, aiming to address phenomena that the original theory cannot fully explain. These modifications strive to provide a deeper insight into the fundamental nature and dynamics of the universe by introducing innovative mathematical concepts and formulations. Some prominent examples of these theories include: $f(R)$ gravity, which extends the Ricci scalar (R) [9][10]. $f(T)$ gravity, formulated via the torsion scalar (T) [11]. $f(G)$ gravity, incorporating the Gauss-Bonnet term (G) [12]. $f(R, \mathbb{T})$ gravity, which combines the scalar R and the trace of the energy-momentum tensor ($\mathbb{T}$) [13]. $f(R, G)$ gravity, uniting the scalar R with the term G [14][15]. $f(Q)$ gravity, focused on the nonmetricity scalar (Q) [16]. $f(Q, T)$ gravity, which merges the scalar Q with the tensor $\mathbb{T}$ [17]. These theories provide a foundation for exploring alternative perspectives on gravitational phenomena and cosmic evolution.

Recently, a groundbreaking theoretical framework called $f(Q, C)$ gravity has been introduced, providing new insights into DE and the universe's accelerating expansion. This theory investigates the nonlinear interplay between the nonmetricity scalar Q and the boundary term C, offering a potential explanation for late-time cosmic acceleration without the need for exotic fields or Λ. The $f(Q, C)$ gravity model is an extension of the $f(Q)$ gravity framework, enhancing the nonmetricity-based approach by introducing a second scalar term, C, which depends on both the Hubble parameter and its time derivative. The additional term C, defined as $C = 6(3H^2 + \dot{H})$, is directly linked to the dynamic aspects of cosmic expansion, particularly the rate of change in the Hubble parameter over time [18][19][20][21]. This feature sets $f(Q, C)$ gravity apart, as it combines the geometric property of nonmetricity (represented by Q) with the evolution of cosmic expansion (captured by C). By incorporating this unique interplay between Q and C within the gravitational action, $f(Q, C)$ gravity is capable of effectively describing both the decelerating and accelerating phases of the universe. The incorporation of C in $f(Q, C)$ gravity introduces new gravitational effects that can be tested via observational data from CMB, large-scale structure (LSS), and SNeIa. In this framework, Q measures deviations in the metric during parallel transport, distinguishing it from GR, which assumes a torsion-free and symmetric connection. The boundary term C, which emerges from the interaction between torsion-free and curvature-free connections, ensures the model's dynamic equivalence to GR under specific conditions, allowing seamless transitions between different geometric representations of gravity. Additionally, C introduces extra degrees of freedom that significantly impact the behavior of gravitational fields, particularly on cosmological scales. In this work, the functional form of $f(Q, C)$ gravity is employed as

$$f(Q, C) = \gamma_1 Q^n + \gamma_2 C, \tag{1}$$

where γ_1, and γ_2 are constants; to maintain nonlinearity, we consider integer $n \geq 1$. The reason behind considering the nonlinear functional form is explained in Section II. [19][22][20][23][24][25][26]. These studies explain the recent work on $f(Q, C)$.

Cosmological observations suggest that the observed accelerated expansion of the universe is a relatively recent phenomenon. During earlier epochs, particularly in the matter-dominated era, when DE was absent or had a negligible effect, the universe must have experienced a decelerated phase to enable the formation of cosmic structures, as gravitational forces held matter together. Consequently, a comprehensive cosmological model must encompass decelerated and accelerated phases of expansion to represent the universe's evolutionary history accurately. In this context, the deceleration parameter serves as a crucial tool. One of the most common ways to achieve such a scenario is through parameterizations of the deceleration parameter, expressed as a function of the scale factor (a), redshift (z), or cosmic time (t) (refer to Refs. [27][28][29][30][31][32]). On the other hand, nonparametric methods, which directly derive the universe's evolution from observational data without assuming specific parameterizations, offer advantages by avoiding constraints on cosmological quantities; they also have certain limitations [33][34][35][36][37]. To date, no theoretical model exists that can fully describe the universe's entire evolution. Therefore, adopting a parametric approach remains a practical choice.

There are several key reasons for adopting such a parameterization. First, it provides a flexible yet controlled approach to studying cosmic evolution, allowing for the exploration of complex dynamics without the need to solve intricate differential equations. Second, parameterized forms are well suited for observational studies, as they enable a direct comparison between theoretical predictions and data from SNeIa, CMB, and BAO [1][38]. Third, they allow for a more intuitive understanding of how the deceleration parameter evolves over cosmic time, capturing key features of cosmological models in terms of a few well-defined parameters [39]. This structured approach enables a detailed investigation of the DE role in cosmic dynamics and its potential implications for modified gravity theories, providing valuable insights into the universe's expansion history.

In the $f(Q, C)$ gravity framework, parameterizing the deceleration parameter ($q(z)$) is particularly beneficial for investigating the implications of cosmic acceleration theories. Unlike the static cosmological constant model, which requires precise fine-tuning. $f(Q, C)$ gravity integrates nonmetricity and dynamic terms that evolve with cosmic time. This combination enables the model to naturally describe the transition between the decelerating and accelerating phases of the universe's expansion. Parameterizing $q(z)$ within this framework provides a structured approach to compare theoretical predictions with empirical data from multiple cosmological probes, such as SNeIa, CMB, and BAO. Notably, many of these parameterizations of $q(z)$ diverge in the far future: whereas others are only valid for low redshift values ($z \ll 1$) [40][41][42][43][44].

Motivated by these considerations, our study adopts parameterization of a specific form of the deceleration parameter:

$$q(z) = q_0 + q_1 \left[\frac{\ln[\alpha + z]}{1 + z} - \beta \right],$$

where q_0, q_1, α, and β are arbitrary model parameters. The logarithmic term is pivotal in capturing the dynamics of $q(z)$. The inclusion of this term ensures smooth and controlled evolution of the deceleration parameter, facilitating a gradual transition between the deceleration and acceleration phases rather than an abrupt shift. This smooth evolution is essential for modeling subtle dynamic changes in the universe's expansion history [45]. Moreover, at high redshifts ($z \gg 1$), the logarithmic term evolves more gradually than the linear terms do, avoiding unphysical divergences and maintaining consistency with early-universe observations [7]. This parameterization significantly enhances the study of the universe's expansion by providing a unified framework to model its evolutionary dynamics. It captures the intricate transition between matter-dominated cosmic deceleration and DE-driven acceleration within a single mathematical expression. Adjusting the model parameters allows for a detailed investigation of the interplay between various cosmic components across different epochs, offering deeper insights into the nature of DE and the mechanisms underlying the universe's accelerated expansion. Furthermore, the controlled and smooth behavior of the logarithmic term ensures alignment with observational constraints from both late-time and early-time cosmological data, making it a robust and versatile tool for understanding the dynamics of cosmic evolution.

This paper examines the parameterization of the deceleration parameter $q(z) = q_0 + q_1 \left[\frac{\ln[\alpha+z]}{1+z} - \beta \right]$ as a function of z. The chosen parameterization exhibits the desired characteristic of transitioning from a decelerating to an accelerating phase. The study investigates the FLRW universe within the framework of $f(Q, C)$ gravity, adopting the functional form $f(Q, C) = \gamma_1 Q^n + \gamma_2 C$. To determine the best-fit values of the model parameters, the chi-square (χ^2) minimization technique is employed. By comparing theoretical predictions with observational data, this study identifies the parameter set that aligns most closely with empirical evidence, facilitated by statistical analysis. The paper is organized as follows: In Section II, we outline the fundamental formalism of $f(Q, C)$ gravity and derive the field equations for the FLRW metric. Section III introduces the parametric form of the deceleration parameter and determines the corresponding Hubble solution. In Section IV, we apply Bayesian analysis to observational datasets, including the Observational Hubble Data (OHD) and $Pantheon + SH0ES$ data, to constrain the free parameters of the model. Section V examined the evolutionary trajectories of energy density, pressure, equation of state (EoS) parameters, statefinder parameters, and the Om diagnostic to demonstrate the universe's accelerating behavior. Finally, section VI summarizes and concludes the results.

II. $f(Q, C)$ gravity and field equations

In GR , the Levi-Civita connection $\overset{\circ}{\Gamma}{}^{\lambda}_{\mu\nu}$ satisfies two important properties: metric compatibility and torsion-free behavior. However, in symmetric teleparallel geometry, these restrictions are removed. Instead, the theory employs a torsion-free and curvature-free affine connection $\Gamma^{\lambda}_{\mu\nu}$, which is symmetric in its lower indices,

justifying the term symmetric teleparallelism. The nonmetricity tensor $Q_{\lambda\mu\nu}$ signifies that the affine connection is not consistent with the metric, which is described by

$$Q_{\lambda\mu\nu} = \nabla_\lambda g_{\mu\nu} = \partial_\lambda g_{\mu\nu} - \Gamma^\beta_{\lambda\mu} g_{\beta\nu} - \Gamma^\beta_{\lambda\nu} g_{\beta\mu} \neq 0. \tag{1}$$

The affine connection can be expressed as a combination of the Levi-Civita connection $\mathring{\Gamma}^\lambda_{\mu\nu}$ and an additional term, the disformation tensor $L^\lambda_{\mu\nu}$ as,

$$\Gamma^\lambda_{\mu\nu} = \mathring{\Gamma}^\lambda_{\mu\nu} + L^\lambda_{\mu\nu} \tag{2}$$

where

$$L^\lambda_{\mu\nu} = \frac{1}{2}(Q^\lambda{}_{\mu\nu} - Q_\mu{}^\lambda{}_\nu - Q_\nu{}^\lambda{}_\mu). \tag{3}$$

Two important nonmetricity vectors are derived from the nonmetricity tensor:

$$Q_\mu = g^{\nu\lambda} Q_{\mu\nu\lambda} = Q_\mu{}^\nu{}_\nu, \quad \tilde{Q}_\mu = g^{\nu\lambda} Q_{\nu\mu\lambda} = Q_{\nu\mu}{}^\nu \tag{4}$$

Similar vectors are also defined from the disformation tensor:

$$L_\mu = L_\mu{}^\nu{}_\nu, \quad \tilde{L}_\mu = L_{\nu\mu}{}^\nu \tag{5}$$

To connect nonmetricity with gravitational dynamics, a superpotential tensor $P^\lambda_{\mu\nu}$, also called the conjugate to nonmetricity, is introduced. It is expressed as:

$$P^\lambda{}_{\mu\nu} = \frac{1}{4}\left(-2L^\lambda{}_{\mu\nu} Q^\lambda g_{\mu\nu} - \tilde{Q}^\lambda g_{\mu\nu} - \delta^\lambda_\mu Q_\nu\right), \tag{6}$$

where parentheses denote symmetrization over indices. Using $P^\lambda{}_{\mu\nu}$, the nonmetricity scalar Q is defined as:

$$Q = Q_{\alpha\beta\gamma} P^{\alpha\beta\gamma}. \tag{7}$$

Owing to the torsion-free and curvature-free properties, certain geometric relationships hold:

$$\mathring{R}_{\mu\nu} + \mathring{\nabla}_\alpha L^\alpha{}_{\mu\nu} - \mathring{\nabla}_\nu \tilde{L}_\mu + \tilde{L}_\alpha L^\alpha{}_{\mu\nu} - L_{\alpha\beta\nu} L^{\beta\alpha}{}_\mu = 0, \tag{8}$$

$$\mathring{R} + \mathring{\nabla}_\alpha(L^\alpha - \tilde{L}^\alpha) - Q = 0. \tag{9}$$

The boundary term C is then introduced to relate the nonmetricity scalar Q to the Ricci scalar $\mathring{R}$ of Levi-Civita geometry. From the above relation, we can also define the boundary term as

$$C = \mathring{R} - Q = -\mathring{\nabla}_\alpha(Q^\alpha - \tilde{Q}^\alpha), \tag{10}$$

where the expression $Q^\alpha - \tilde{Q}^\alpha = L^\alpha - \tilde{L}^\alpha$ indicates that the boundary term C represents the difference between the nonmetricity vectors. This formulation highlights that C encapsulates not only the difference between the Ricci scalar $\mathring{R}$ and the nonmetricity scalar Q but also illustrates their relationship through the divergence of the nonmetricity vector differences. Fundamentally, this establishes a link between the geometric structure of spacetime and the behavior of the nonmetricity vectors, demonstrating how variations in nonmetricity influence the curvature within the framework of the theory.

The action for $f(Q, C)$ gravity is defined as:

$$S = \int \left[\frac{1}{2\kappa} f(Q,C) + \mathcal{L}_m \right] \sqrt{-g} d^4 x, \tag{11}$$

where $f(Q,C)$ is a general function of the nonmetricity scalar Q and boundary term C, $\kappa = \frac{8\pi G}{c^4}$ is the coupling constant, and $\mathcal{L}_m$ represents the matter Lagrangian, and $\sqrt{-g} = \det(e^A_\mu) = e$.

Varying the action to the metric yields the field equations:

$$\kappa T_{\mu\nu} = -\frac{f}{2} g_{\mu\nu} + \frac{2}{\sqrt{-g}} \partial_\lambda \left(\sqrt{-g} f_Q P^\lambda{}_{\mu\nu} + \left(P_{\mu\alpha\beta} Q_\nu{}^{\alpha\beta} - 2P_{\alpha\beta\nu} Q^{\alpha\beta}{}_\mu \right) f_Q +$$
$$\left(\frac{C}{2} g_{\mu\nu} - \mathring{\nabla}_\mu \mathring{\nabla}_\nu + g_{\mu\nu} \mathring{\nabla}^\alpha \mathring{\nabla}_\alpha - 2P^\lambda{}_{\mu\nu} \partial_\lambda \right) f_C. \tag{12}$$

For a detailed demonstration of this equation, one can refer to [46]. The covariant form is given as

$$\kappa T_{\mu\nu} = -\frac{f}{2} + 2P^\lambda{}_{\mu\nu} \nabla_\lambda (f_Q - f_c) + \left(\mathring{G}_{\mu\nu} + \frac{Q}{2} g_{\mu\nu} \right) f_Q +$$
$$\left(\frac{C}{2} g_{\mu\nu} - \mathring{\nabla}_\mu \mathring{\nabla}_\nu + g_{\mu\nu} \mathring{\nabla}^\alpha \mathring{\nabla}_\alpha \right) f_C, \tag{13}$$

where $\mathring{G}_{\mu\nu}$ is an Einstein tensor corresponding to the Levi-Civita connection. An effective energy-momentum tensor $T_{\mu\nu}^{\text{eff}}$ is introduced to simplify the equations. This tensor accounts for the geometric modifications and generates additional terms, mimicking the effects of DE:

$$T_{\mu\nu}^{\text{eff}} = T_{\mu\nu} + \frac{1}{\kappa} \left[\frac{f}{2} g_{\mu\nu} - 2P^\lambda{}_{\mu\nu} \nabla_\lambda (f_Q - f_C) - \frac{Q f_Q}{2} g_{\mu\nu} - \left(\frac{C}{2} g_{\mu\nu} - \mathring{\nabla}_\mu \mathring{\nabla}_\nu + g_{\mu\nu} \mathring{\nabla}^\alpha \mathring{\nabla}_\alpha \right) f_C \right]. \tag{14}$$

Using the above equation, we derive an equation analogous to that in GR as follows:

$$\mathring{G}_{\mu\nu} = \frac{\kappa}{f_Q} T_{\mu\nu}^{\text{eff}}. \tag{15}$$

We consider the energy-momentum tensor of a perfect fluid to be:

$$T_{\mu\nu} = p g_{\mu\nu} + (\rho + p) u_\mu u_\nu, \tag{16}$$

where ρ is the energy density, p is the pressure and u^μ represents the four velocities of the fluid.

In this theory, where the affine connection is considered an independent entity, the connection field equation is derived by varying the action with respect to the affine connection.

$$(\nabla_\mu - \widetilde{L}_\mu)(\nabla_\nu - \widetilde{L}_\nu)[4(f_Q - f_C)P^{\mu\nu}{}_\lambda + \nabla_\lambda{}^{\mu\nu}] = 0, \tag{17}$$

where

$$\nabla_\lambda{}^{\mu\nu} - \frac{2}{\sqrt{g}} \frac{\delta(\sqrt{-g}\mathcal{L}_m)}{\delta\Gamma^\lambda{}_{\mu\nu}}$$

The cosmological principle states that, on large scales, the universe is homogeneous and isotropic. This assumption leads to the widely used Friedmann−Lemaître−Robertson−Walker (FLRW) metric, which describes a spatially flat universe. In Cartesian coordinates, the FLRW metric is expressed as:

$$ds^2 = -dt^2 + a^2(t)(dx^2 + dy^2 + dz^2), \tag{18}$$

where $a(t)$ is the scale factor determining the universe's expansion. The Hubble parameter, which measures the rate of expansion, is defined as $H(t) = \frac{\dot{a}}{a}$, where the overdot ($\dot{a}$) represents the derivative for cosmic time t.

As demonstrated in the previous section, the framework of $f(Q, C)$ gravity introduces an additional, effective sector of geometric origin, as expressed in Eqn. (14). In a cosmological context, this extra term can be interpreted as an effective DE component characterized by its corresponding energy-momentum tensor.

$$T_{\mu\nu}^{\text{DE}} = \frac{1}{f_Q}\left[\frac{f}{2}g_{\mu\nu} - 2P^\lambda{}_{\mu\nu}\nabla_\lambda(f_Q - f_C) - \frac{Qf_Q}{2}g_{\mu\nu} - \left(\frac{C}{2}g_{\mu\nu} - \mathring{\nabla}_\mu\mathring{\nabla}_\nu + g_{\mu\nu}\mathring{\nabla}^\alpha\mathring{\nabla}_\alpha\right)f_C\right] \qquad (19)$$

Fundamental to all modified gravity theories, this additional $T_{\mu\nu}^{\text{DE}}$ component essentially produces negative pressure, which drives the late-time acceleration of the universe.

The Lie derivatives of the connection coefficients concerning the generating vector fields of spatial rotations and translation vanish in a symmetric teleparallel affine connection, which is a torsion-free, curvature-free affine connection with both spherical and translational symmetries. In the context of $f(Q, C)$ gravity, we work with a vanishing affine connection, $\Gamma^\alpha{}_{\mu\nu} = 0$. To explore this setup in greater detail, refer to [47], and the following quantities are derived:

$$\mathring{G}_{\mu\nu} = -\left(3H^2 + 2\dot{H}\right)h_{\mu\nu} + 3H^2 u_\mu u_\nu, \quad \mathring{R} = 6\left(2H^2 + \dot{H}\right), \quad Q = -6H^2, \quad C = 6\left(3H^2 + \dot{H}\right), \quad (20)$$

where $u_\nu = (dt)_\nu$, $h_{\mu\nu} = g_{\mu\nu} + u_\mu u_\nu$. The modified Friedmann-like equations in $f(Q, C)$ gravity are obtained by introducing these quantities in the general field equation (12) as

$$3H^2 = \kappa\left(\rho_m + \rho_{DE}\right), \qquad (21)$$

$$-\left(2\dot{H} + 3H^2\right) = \kappa\left(p_m + p_{DE}\right), \qquad (22)$$

where ρ_m and p_m are the energy density and pressure of the matter sector, respectively. The effective DE density and pressure are defined as

$$\kappa\rho_{DE} = -\frac{f}{2} + 3H^2\left(1 - 2f_Q\right) + \left(9H^2 + 3\dot{H}\right)f_C - 3H\dot{f}_C, \qquad (23)$$

$$\kappa p_{DE} = \frac{f}{2} - 2\dot{H}\left(1 - f_Q\right) - 3H^2\left(1 - 2f_Q\right) + 2H\dot{f}_Q - \left(9H^2 + 3\dot{H}\right)f_C + \ddot{f}_C, \qquad (24)$$

where $f_Q = \partial f/\partial Q$ and $f_C = \partial f/\partial C$ are partial derivatives of the function $f(Q, C)$ concerning Q and C, respectively. The derivatives $\dot{f}_C$ and $\ddot{f}_C$ represent time derivatives of f_C. These equations generalize the standard FLRW equations of general relativity by incorporating the additional contributions from the Q and C dependent terms in the $f(Q, C)$ gravity. The first equation corresponds to the energy constraint, whereas the second governs the dynamics of the universe's expansion.

III. Parametrizing the Deceleration Parameter

In general, the deceleration parameter $q(z)$ in terms of $H(z)$ is given as

doi.org/10.32388/N3VJIS

$$q(z) = -1 + \frac{(1+z)}{H(z)} H',$$ (25)

where $H' = \frac{dH(z)}{dz}$. The parameterization of the deceleration parameter significantly influences the nature of the universe's expansion. Some studies used a variety of parametric forms of deceleration parameters in this regard, whereas others looked at nonparametric forms. These techniques have been extensively addressed in the literature to characterize issues with cosmological inquiries, including the Hubble tension, the initial singularity problem, the horizon problem, the all-time decelerating expansion problem, and others[48][41][49]. Inspired by this finding, we analyze the parametric form of the deceleration parameter in terms of redshift z in this article as:

$$q(z) = q_0 + q_1 F(z),$$ (26)

where q_0 and q_1 are free parameters, whereas $F(z)$ is a function of z. Several functional forms of $F(z)$ have been presented[41][50][51][52][53][54], which can satisfactorily address several cosmological issues. However, as already established, some of these parameters lose their power to forecast how the universe will evolve in the future, whereas others are only applicable for $z \ll 1$. Moreover, *A.A. Mamon et al.* investigated the divergence-free parameterization of $q(z)$ to study the universe's expansion history[55]. They demonstrated that such a model is more in line with the existing observational constraints for certain model parameter restrictions. Therefore, efforts are being made to find a suitable functional form of $q(z)$ that will work well to address cosmological issues. Inspired by these facts, we adapt a parameterization of the deceleration parameter in this article, which is provided by

$$q(z) = q_0 + q_1 \left[\frac{\log[\alpha + z]}{1+z} - \beta \right],$$ (27)

where α and β are arbitrary model parameters. Equation (27) shows two limiting conditions.

- At the early epoch. i.e., $z \to \infty \implies q(z) = q_0 - \beta q_1$
- At the current epoch. i.e., $z = 0 \implies q(z) = q_0 + q_1 \log[\alpha - \beta]$

We derive the differential equation by solving Eqns. (25) and (27). On further calculations, we obtained

$$H(z) = \left[(\alpha + z)^{-\frac{q_1}{1+z}} \left(\frac{\alpha + z}{1+z} \right)^{\frac{q_1}{\alpha-1}} (1+z)^{1+q_0-\beta q_1} C^* \right],$$ (28)

where C^* is the integrating constant. Furthermore, to eliminate C^*, we assume a boundary condition, i.e., $z = 0$. When solving (28), we, obtain

$$H_0 = \alpha^{-\frac{q_1 \alpha}{\alpha-1}} C^*$$ (29)

where H_0 is the Hubble value/constant at $z = 0$. After substituting this value in (28), the expression for the Hubble parameter $H(z)$ is obtained as

$$H(z) = H_0 \left[\alpha^{\frac{q_1 \alpha}{\alpha-1}} (\alpha + z)^{-\frac{q_1}{1+z}} \left(\frac{\alpha + z}{1+z} \right)^{\frac{q_1}{\alpha-1}} (1+z)^{1+q_0-\beta q_1} \right]$$ (30)

Now we consider the nonlinear $f(Q, C)$ model as:

$$f(Q, C) = \gamma_1 Q^n + \gamma_2 C, \tag{31}$$

where γ_1, γ_2 and n are constants. The choice of a nonlinear form over a linear form of $f(Q, C)$ gravity has been thoroughly justified in the literature[22]. The dynamical system in $f(Q)$ gravity theory was thought to be analyzed by *Rana et al.*[56] in the form $f(Q, C) = -Q + \gamma_1 Q^n$. In contrast, *D.C. Maurya* examined the $f(Q, C) = \gamma Q^2 + \gamma_2 C^2$ form to examine the quintessence behavior in $f(Q, C)$ gravity theory[23]. Several authors have used a variety of nonlinear forms in various gravity theories. Motivated by the models mentioned earlier, we consider this specific nonlinear form in our computations.

IV. Data Interpretation

This section outlines the methodologies and the selection of observational datasets utilized to constrain the parameters H_0, q_0, q_1, α, and β in the proposed cosmological model. The posterior distributions of these parameters are derived through statistical analysis, specifically employing the Markov Chain Monte Carlo (MCMC) technique. For the data analysis, the Python module emcee is used.

The probability function $\mathcal{L} \propto \exp(-\chi^2/2)$ is employed to optimize the parameter fit, where χ^2 denotes the pseudo-Chi-squared function[57]. Details of the χ^2 function for various data samples are discussed in the subsequent subsections. The MCMC plot features 1-D curves for each model parameter, obtained by marginalizing over the remaining parameters. The thick-line curve represents the best-fit value. The diagonal panels of the plot show these 1-D distributions, whereas the off-diagonal panels illustrate 2-D projections of the posterior probability distributions for parameter pairs. These panels include contours highlighting the regions corresponding to the 1-σ and 2-σ confidence levels.

A. Observed Hubble Data

Accurately determining the expansion rate as a function of cosmic time t is challenging. The cosmic chronometers (CC) method offers a distinctive and potentially valuable approach because the expansion rate can be expressed as $H(z) = \dot{a}/a = -[1/(1+z)]dz/dt$. In this method, only the differential age progression of the universe, Δt, within a specific redshift interval Δz, needs to be measured, as Δz is obtained from high-precision spectroscopic surveys. From the ratio $\Delta z/\Delta t$, an approximate value for dz/dt can be determined.

To estimate the model parameters, we utilize 31 data points from the $H(z)$ datasets derived via the differential age (DA) technique, spanning the redshift range $0.07 < z < 2.42$. The complete list of this dataset is compiled in[58]. The Chi-square function used for deducing the model parameters is as follows:

$$\chi^2_{CC} = \sum_{i=1}^{31} \left[\frac{H_i^{th}(\Theta_s, z_i) - H_i^{obs}(z_i)}{\sigma_{H(z_i)}} \right]^2, \tag{32}$$

here, H^{th} and H^{obs} represent the theoretical and observed values of the Hubble parameter, respectively. The parameter set $\Theta_s = (H_0, q_0, q_1, \alpha, \beta)$ defines the cosmological background parameter space. The standard deviation of the ith data point is denoted by $\sigma_{H(z_i)}$. Figure 1 shows the Hubble parameter profile derived from the CC dataset alongside the behavior predicted by the ΛCDM model. For the MCMC analysis, we employed 100 walkers and 10,000 steps to obtain the fitting results. Contour plots showing the 1-σ and 2-σ confidence levels are provided in Figure 2. While the model closely aligns with the ΛCDM paradigm at low redshift, noticeable deviations appear at higher redshifts. The marginal values of all the model parameters derived from the Hubble dataset are summarized in Table 1.
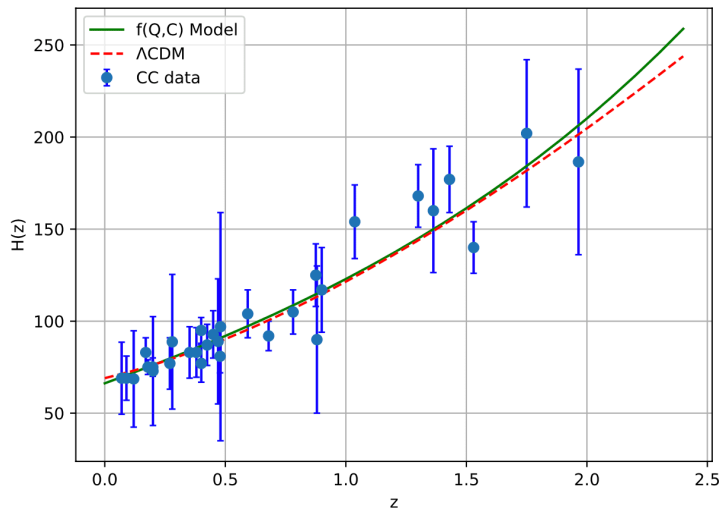
Figure 1. Error bar plots for 31 data points from the Hubble datasets, together with best-fit plots.
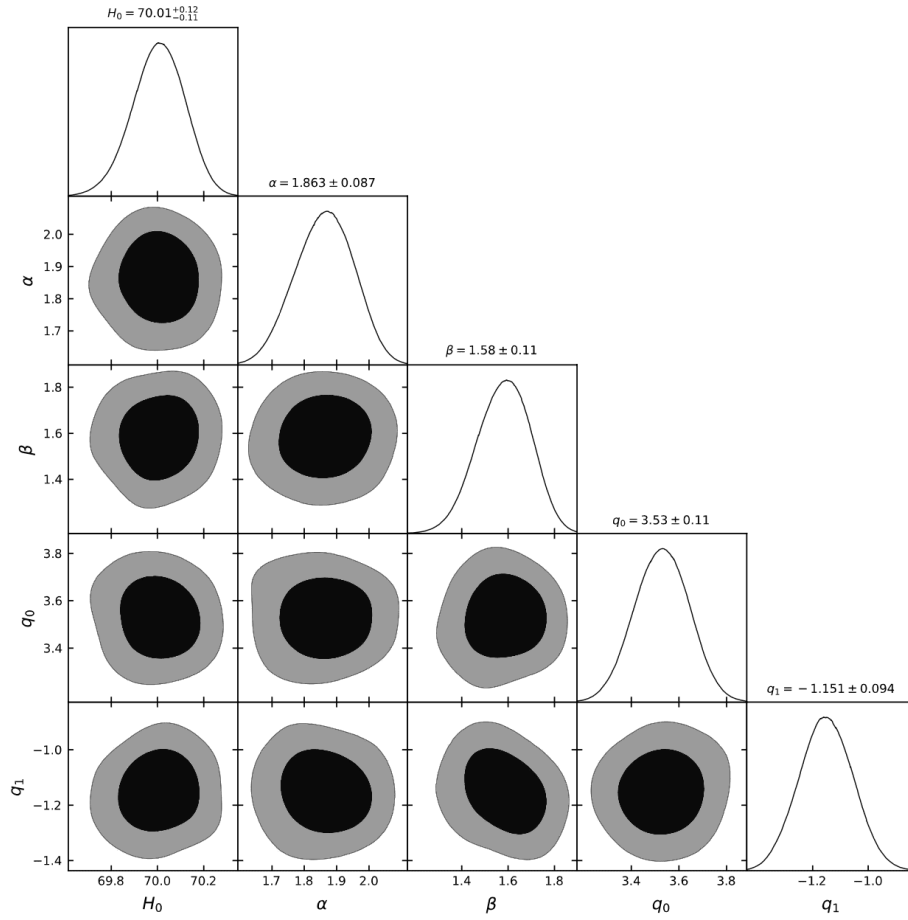
Figure 2. Marginalized constraints on the coefficients in the expression of $H(z)$ in Eqn. 28 are shown by using the Hubble sample

Parameters	OHD	$Pantheon + SH0ES$
H_0	$70.01^{+0.12}_{-0.11}$	70.01 ± 0.11
α	1.863 ± 0.087	1.864 ± 0.099
β	1.58 ± 0.11	1.61 ± 0.10
q_0	3.53 ± 0.11	3.53 ± 0.10
q_1	-1.151 ± 0.094	$-1.14^{+0.11}_{-0.12}$

Table 1. Constrained values of the model parameters obtained from the OHD and $Pantheon + SH0ES$ data samples

B. *Pantheon + SH0ES Data*

The discovery of the accelerated expansion of the universe has been significantly advanced through observations of SNeIa. SNeIa has proven to be one of the most powerful tools for investigating the properties of the components driving the universe's rapid evolution. In recent years, numerous compilations of SNeIa data, such as the Joint Light-Curve Analysis (JLA), Pantheon, Pantheon+, Union, Union 2, and Union 2.1[59][60][61][62][63], have been published. The *Pantheon + SH0ES* dataset consists of 1701 light curves from 1550 distinct SNeIa , covering redshifts from $z = 0.00122$ to 2.2613. To constrain the model parameters, the observed and theoretical distance modulus values must be compared. The theoretical distance modulus, μ_i^{th}, is expressed as:

$$\mu_i^{\text{th}}(z, \theta) = 5 \log D_l(z, \theta) + 25, \tag{33}$$

where D_l is the dimensionless luminosity distance defined as,

$$D_l(z, \theta) = (1 + z) \int_0^z \frac{d\bar{z}}{H(\bar{z})}. \tag{34}$$

Now, the Chi-square function is defined as:

$$\chi_{\text{SN}}^2(z, \theta) = \sum_{i,j=1}^{1701} \nabla \mu_i \, (C_{\text{SN}}^{-1})_{ij} \, \nabla \mu_j, \tag{35}$$

$\nabla \mu_i = \mu_i^{\text{th}}(z, \theta) - \mu_i^{\text{obs}}$ represents the difference between the theoretical and observed distance moduli. The observed distance modulus is denoted as μ_i^{obs}, where θ defines the parameter space and C_{SN} is the covariance matrix[64].

The MCMC analysis was conducted using the same number of steps and walkers as in the CC example. Figure 3 presents the distance modulus profile, whereas Figure 4 displays the 1-σ and 2-σ confidence level contour plots. The model shows excellent agreement with the *Pantheon + SH0ES* dataset. The marginal values of all the model parameters obtained via this dataset are listed in Table 1.
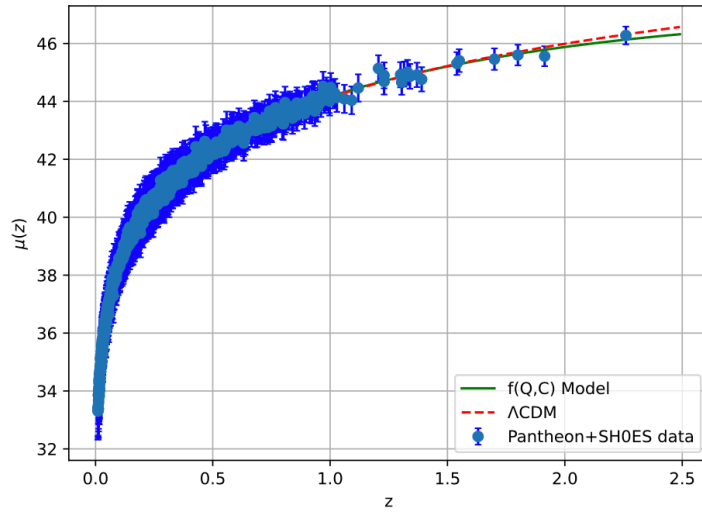
Figure 3. Error bar plots for 1701 data points from the

$Pantheon + SHE0ES$ datasets together with best–fit plots.
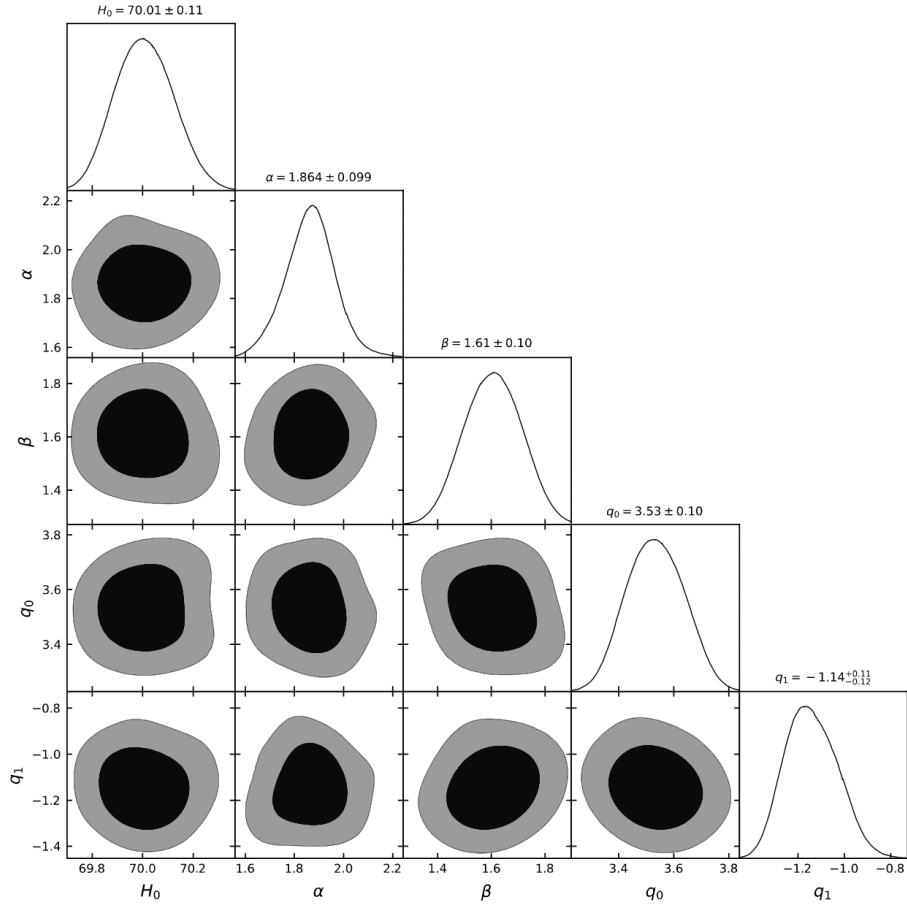
Figure 4. The MCMC confidence contours derived from constraining the $f(Q, C)$ model via $Pantheon + SH0ES$ dataset are shown in the plot.

Datasets	q_0	z_t	ω_0
OHD	$-0.2815^{+0.25}_{-0.15}$	$0.98^{+0.007}_{-0.066}$	$-0.545^{+0.49}_{-0.66}$
$Pantheon + SH0ES$	$-0.2584^{+0.26}_{-0.28}$	$0.76^{+0.012}_{-0.048}$	$-0.695^{+0.46}_{-0.56}$

Table 2. Best-fit values of the cosmological parameters and statistical analysis results for the OHD and $Pantheon + SH0ES$ datasets, including confidence levels.

V. Cosmographic parameters

A. Deceleration parameter

The deceleration parameter q measures the rate at which the universe's expansion changes over t, or z. A positive $q(z)$ signifies a decelerated expansion, typically associated with matter or radiation dominance. In contrast, a negative value indicates accelerated expansion, as seen in the present DE-dominated universe. Tracking its behavior helps in understanding the impact of different cosmic components on the universe's expansion. The equation for $q(z)$, obtained from the parametrically derived $H(z)$ Eqn. (30), is given by:

$$q(z) = \frac{1}{(1+z)(\alpha-1)} \left[(1+z) \left[2 + q_0(\alpha-1)^2 + \alpha(\alpha+q_1-3) - q_1(\alpha-1)^2\beta \right] + (q_1 - \alpha q_1)\log[\alpha+z] \right] \quad (36)$$

Figure 5 depicts the universe's evolution, highlighting its transition from early-time deceleration to late-time acceleration, as determined by the constrained values of the model parameters derived from the observational data used in this article. The transition redshifts are obtained as $z_t \approx 0.98$ and, $z_t \approx 0.76$ for the OHD and $Pantheon + SH0ES$ datasets, respectively. The OHD clearly indicates a delayed transition for cosmic acceleration. The current values of the deceleration parameter for the OHD and $Pantheon + SH0ES$ samples are observed to be $q_0 \approx -0.30$ and $q_0 \approx -0.25$, respectively. This confirms that the universe is undergoing accelerated expansion, with the negative values highlighting the dominance of DE in the current epoch. From these values, it is evident that the model initially struggles to align with the widely accepted value of $q_0 \approx -0.55$. However, as it evolves, the model may successfully transition into an accelerating de Sitter regime.
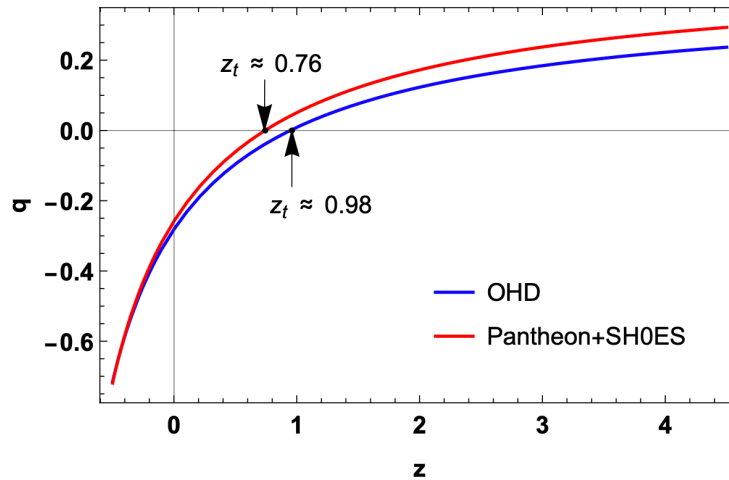
Figure 5. Plot of deceleration parameter $q(z)$ versus redshift z

B. Density and pressure

With the help of Eqns. (23), (24) and (31), the energy density and pressure for the derived DE model are given as

$$\rho_{DE} = \frac{1}{\kappa}\left[3H^2 + \gamma_1(n - 0.5)(-6H^2)^n\right], \tag{37}$$

$$p_{DE} = -\frac{1}{\kappa}\left[2\dot{H} + 3H^2 + \gamma_1(n - 0.5)(-6H^2)^n + \frac{\gamma_1 n(2n - 1)\dot{H}}{3}(-6)^n(H^2)^{n-1}\right]. \tag{38}$$

The value of γ_1 determines how ρ_{DE} and p_{DE} are expressed. This suggests that the nonmetricity factor Q directly impacts the obtained model. To preserve a positive energy density and the accelerating features of the EoS parameter, We then set the values of our model parameters, γ_1 and γ_2, appropriately. Additionally, an integer value of $n \geq 1$ is required to achieve valid results for noninteger values, given that the model does not correlate correctly. The model parameters, q_0, q_1, α, and β, affect the energy density and pressure of the DE model. Therefore, we use $\gamma_1 = 0.235$ and $n = 2$, to keep the Hubble and deceleration parameters within the ranges suggested by cosmological discoveries.

Figure 6 presents the evolution of the DE density ρ_{DE} as a function of redshift z. At low redshifts ($z \approx 0$), the results from both datasets demonstrate similar trends in energy density, which approaches near–zero values. This behavior aligns with the current epoch of accelerated cosmic expansion, which is dominated by DE or low–density matter. At higher redshifts, the energy density ρ_{DE} exhibits exponential growth, with the $Pantheon + SH0ES$ dataset predicting slightly higher values than the OHD dataset does. This indicates a denser universe in the past, particularly for redshifts ($z > 2$). As the redshift approaches ($z \to -1$), DE density ρ_{DE} appears to stabilize or entirely dominate, in agreement with the theoretical expectations of an accelerating de Sitter universe.
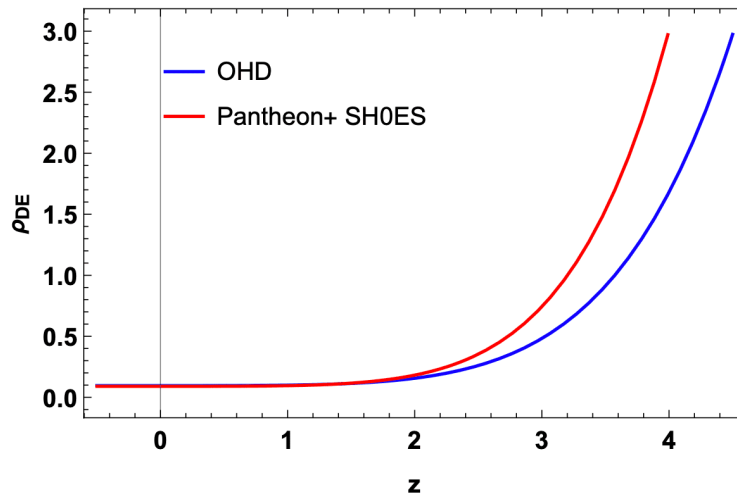
Figure 6. Plot of energy density ρ versus redshift z

Figure 7 shows the variation in DE pressure p_{DE} as a function of redshift z for two datasets: OHD and $Pantheon + SH0ES$. The plot illustrates the evolution of pressure across different cosmic epochs. In the past ($z > 0$), corresponding to the early universe, the pressure was highly negative, with the $Pantheon + SH0ES$ dataset showing a steeper decline than the OHD datset. This indicates a stronger influence of DE in the $Pantheon + SH0ES$ dataset during earlier times, suggesting a more rapid expansion of the universe. At present ($z \approx 0$), both datasets converge to less negative pressure values, which is consistent with the current accelerated expansion dominated by DE and low-density matter. Looking toward the future ($z \to -1$), although the figure does not explicitly extend into this regime, the pressure is expected to stabilize near zero or remain negative, aligning with the universe transitioning into a de Sitter phase.
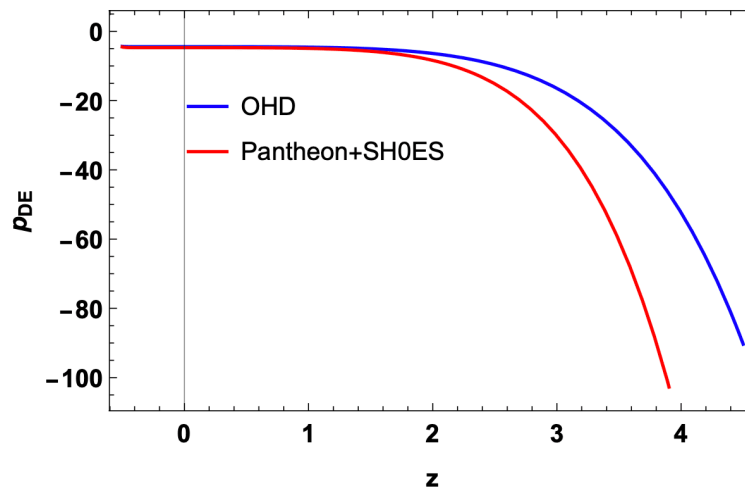
Figure 7. Plot of pressure p versus redshift z

C. The EoS parameter
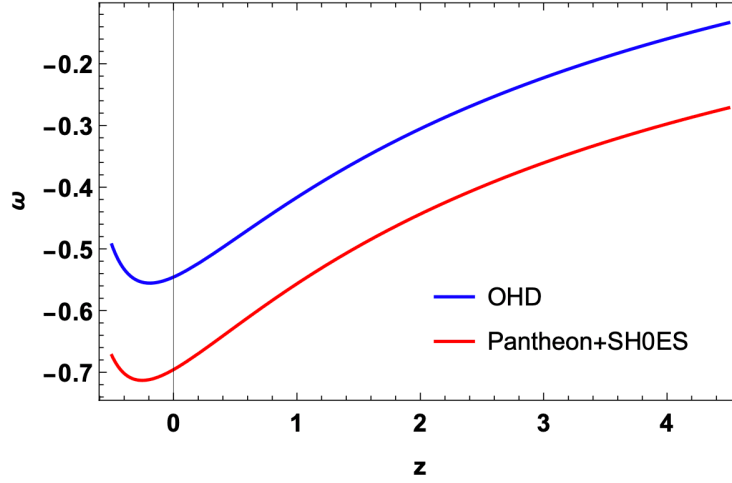
Figure 8. Plot of the EoS parameter ω versus redshift the z

The EoS parameter ω, which is defined as $\omega = \frac{p_{DE}}{\rho_{DE}}$, is useful for classifying the universe's acceleration and decelerating behavior. To accelerate the universe, the EoS classifies three possible states: the cosmological constant ($\omega = -1$), phantom ($\omega < -1$) era, and quintessence ($-1 < \omega < -\frac{1}{3}$) era. Figure 8 explains the trajectory of EoS parameter. It indicates that ω ranges between -1 to $-\frac{1}{3}$, throughout the evolution, which means that the whole trajectory lies in the quintessence era. The current values of the EoS parameter for OHD and $Pantheon + SH0ES$ are observed to be $\omega_0 \approx -0.55$ and, $\omega_0 \approx -0.70$, respectively.

D. $r - s$ parameter

It is well known that DE promotes the expansion of the universe. Understanding the origins and basic characteristics of DE have gained attention in recent decades. Consequently, many DE models have surfaced, underscoring the necessity of making both quantitative and qualitative distinctions between them. To distinguish between several DE theories, *Sahni et al.*[65] presented a statefinder diagnostic technique. The statefinder parameter $\{r, s\}$, a pair of geometrical parameters used in this approach, are specified as follows:

$$r = 2q^2 + q + (1+z)\frac{dq}{dz},$$ (39)

$$s = \frac{r - 1}{3(q - \frac{1}{2})}.$$ (40)

The DE models are represented by different values of (r, s); for example, the ΛCDM model is represented by $(r = 1, s = 0)$, the Chaplygin gas region is represented by $(r > 1, s < 0)$, and the Quintessence region is represented by $(r < 1, s > 0)$. Figure 9 illustrates the trajectory of the $r - s$ parameter for the OHD and

$Pantheon + SH0ES$ datasets. This indicates that $r - s$ the pair falls within the Chaplygin gas regime $(r > 1, s < 0)$ and eventually converges to the ΛCDM point $(0, 1)$.
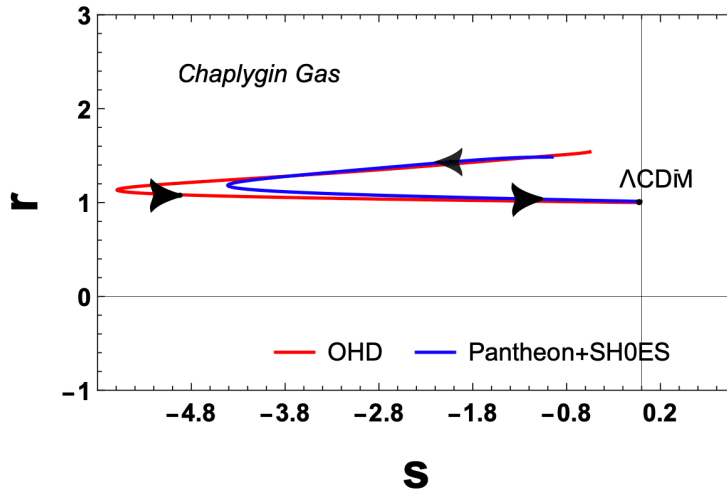
Figure 9. Plot of $r - s$ parameter versus redshift z

E. $Om(z)$ diagnostics
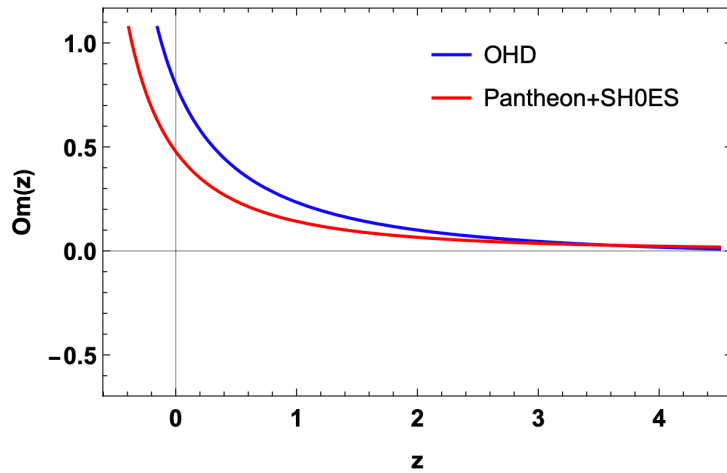
Figure 10. Plot of Om diagnostic $Om(z)$ versus redshift z

Hubble parameter H and redshift z provide the geometrical diagnosis known as Om. It can distinguish between a dynamic DE model and ΛCDM, both with and without matter density. The negative slope of $Om(z)$ indicates that DE behaves like a quintessence $(\omega > -1)$, the positive slope suggests that DE is a phantom $(\omega < -1)$. Following Zunckel & Clarkson [66] and Sahni et al. [67], $Om(z)$ for a spatially flat universe is defined as

$$Om(z) = \frac{[H(z)/H_0]^2 - 1}{(1+z)^3 - 1}. \tag{41}$$

Figure 10 shows that $Om(z)$ has a negative slope, which denotes the quintessence-like behavior of DE, in a slowly evolving equation of state for both datasets.

VI. Conclusion

The present theory of the universe's accelerating expansion has become more exciting over time. To find a good representation of the accelerating universe, many dynamic DE models and modified gravity theories have been used in different ways. In this work, we employ an extension $f(Q)$ gravity, along with a boundary term C., i.e., $f(Q, C)$ gravity. The nonlinear functional form $f(Q, C)$ gravity is shown by Eqn. (31). We execute the parameterization of the logarithmic deceleration parameter Eqn. (27) with the help of $f(Q, C)$ gravity in the FLRW universe. The optimal results are determined via the χ^2 minimization method to identify the best-fit values for the model parameters α, β, q_0, and q_1. This process involves the use of data samples, mainly 31 data points from the CC dataset for Hubble measurement and 1701 data points from the $Pantheon + SH0ES$ dataset for SNeIa. Table 1 presents the constrained parameter values along with their corresponding 1-σ confidence intervals. Additionally, Table 2 provides the best-fit values of the cosmological parameters for the current epoch. We compute and study cosmographic parameters, such as the deceleration parameter, pressure, energy density of the DE model, effective EoS parameter, statefinder parameter, and Om diagnostic.

Figure 1.S shows the trajectory of the Hubble parameter, which indicates that it aligns well with the standard ΛCDM model. The current values of the Hubble parameter H_0 for the OHD and $Pantheon + SH0ES$ data samples are $H_0 = 70.01^{+0.12}_{-0.11} kms^{-1} Mpc^{-1}$ and $H_0 = 70.01 \pm 0.11 kms^{-1} Mpc^{-1}$ respectively, which are similar to the results of [68][69]. The behavior of the deceleration parameter is shown in Figure 5. At higher redshifts, where q has positive values, the model exhibits a decelerating phase. Upon crossing the transition redshift values, $z_t = 0.98^{+0.007}_{-0.066}$ for the OHD dataset and $z_t = 0.76^{+0.012}_{-0.048}$ for the $Pantheon + SH0ES$ dataset, the model transitions into an accelerated phase at lower redshifts. As the model continues to evolve, it is expected to eventually transition successfully into an accelerating de Sitter phase soon. The current values of the deceleration parameter for each dataset are provided in Table 2. These results align closely with the arguments presented in [70][46].

The energy density ρ_{DE} experiences a steady decline from its high values in the early universe ($z > 0$) to nearly zero as we approach the future ($z < 0$) (Figure 6). This behavior corresponds with the transition from a radiation-dominated era to a vacuum-dominated, de Sitter-like phase, highlighting the model's effectiveness in accounting for the diminishing influence of matter and radiation as the universe expands. These findings are consistent with the reasoning outlined in [69][71][72].

In parallel, the DE pressure p_{DE} shifts from significantly negative values in the early universe to values near zero in the later stages, as depicted in Figure 7. This trend mirrors the dynamics of accelerated expansion promoted by

DE. The increasing negativity of pressure further underscores the importance of $f(Q,C)$ gravity in representing the repulsive forces essential for cosmic acceleration. These outcomes support similar conclusions as those reported in [73][74].

The equation of the state parameter ω (Figure 8) exhibits negative behavior, indicating that it lies within the quintessence era. This behavior suggests that the present universe is undergoing an accelerating phase, reinforcing the notion that DE plays a significant role in its dynamics. It does not cross the phantom divide line for $(z < 0)$ for each dataset. The current values of the Eos parameter are $\omega_0 = -0.545^{+0.49}_{-0.66}$ for OHD and $\omega_0 = -0.695^{+0.46}_{-0.56}$ for $Pantheon + SH0ES$ data samples. These results align closely with the arguments presented in [75][76][77].

The statefinder $r-s$ parameter for constrained values of model parameters, derived from the OHD and $Pantheon + SH0ES$ data samples, is presented in Figure 9. Initially, the trajectory of the $r-s$ plane is positioned in the region where $r > 1$ and $s < 0$, which is typically associated with Chaplygin gas. As the model evolves, the pair (r,s) converges toward $(1,0)$, aligning it with the widely accepted ΛCDM model. These results are in agreement with the results highlighted in [78][79][80].

In Figure 10, the evolution of the $Om(z)$ diagnostic is clearly depicted with a negative slope. This suggests that our model aligns with the quintessence phase of DE for each dataset, characterized by a slowly evolving equation of state. This finding is consistent with theoretical expectations for quintessence, where DE is dynamic and evolves, in contrast to the static nature of the cosmological constant. These results correspond well with the arguments discussed in [81][76][82].

To summarize, the choice of $q(z)$ Eqn. 25 with a logarithmic term is somewhat arbitrary and is adopted here to explore the impact of the logarithmic term on the resulting cosmological model and its parameters. This assumption also helps close the system of equations. Since the true nature of the universe remains elusive, parameterizing $q(z)$ offers a simple yet effective approach to studying the universe's transition from a decelerating to an accelerating expansion phase, while paving the way for future investigations into the properties of DE. Incorporating additional observational datasets into this analysis would undoubtedly improve the accuracy of constraints on the universe's expansion history, positioning this work as a foundational step in that direction. Furthermore, the $f(Q,C)$ gravity framework provides a unified explanation of the universe's physical behavior across its early, current, and late stages. By analyzing the dynamics of isotropic pressure, energy density, stability parameters, and energy conditions. This model offers a comprehensive alternative to ΛCDM.

Statements and Declarations

Data Availability

There are no new data associated with this article.

References

1. [a, b]A. G. Riess, A. V. Filippenko, P. Challis, A. Clocchiatti, A. Diercks, P. M. Garnavich, R. L. Gilliland, C. J. Hogan, S. Jha, R. P. Kirshner, et al. (1998) Observational evidence from supernovae for an accelerating universe and a cosmological constant. The astronomical journal 116 (3), pp. 1009. Cited by: §I, §I.

2. [^]S. Perlmutter (2003) Dark energy: recent observations and future prospects. Philosophical Transactions of the Roya l Society of London. Series A: Mathematical, Physical and Engineering Sciences 361 (1812), pp. 2469–2478. Cited by: §I.

3. [^]T. Clifton, P. G. Ferreira, A. Padilla, and C. Skordis (2012) Modified gravity and cosmology. Physics reports 513 (1-3), pp. 1–189. Cited by: §I.

4. [^]A. G. Riess, S. Casertano, W. Yuan, L. M. Macri, and D. Scolnic (2019) Large magellanic cloud cepheid standards prov ide a 1% foundation for the determination of the hubble constant and stronger evidence for physics beyond λ cdm. T he Astrophysical Journal 876 (1), pp. 85. Cited by: §I.

5. [^]S. Weinberg (1989) The cosmological constant problem. Reviews of modern physics 61 (1), pp. 1. Cited by: §I.

6. [^]P. J. Steinhardt, L. Wang, and I. Zlatev (1999) Cosmological tracking solutions. Physical Review D 59 (12), pp. 12350 4. Cited by: §I.

7. [a, b]E. J. Copeland, M. Sami, and S. Tsujikawa (2006) Dynamics of dark energy. International Journal of Modern Phys ics D 15 (11), pp. 1753–1935. Cited by: §I, §I.

8. [^]L. Amendola and S. Tsujikawa (2010) Dark energy: theory and observations. Cambridge University Press. Cited by: §I.

9. [^]H. A. Buchdahl (1970) Non-linear lagrangians and cosmological theory. Monthly Notices of the Royal Astronomica l Society 150 (1), pp. 1–8. Cited by: §I.

10. [^]A. A. Starobinsky (1980) A new type of isotropic cosmological models without singularity. Physics Letters B 91 (1), p p. 99–102. Cited by: §I.

11. [^]R. Ferraro and F. Fiorini (2007) Modified teleparallel gravity: inflation without an inflaton. Physical Review D—Pa rticles, Fields, Gravitation, and Cosmology 75 (8), pp. 084031. Cited by: §I.

12. [^]S. Nojiri and S. D. Odintsov (2005) Modified gauss–bonnet theory as gravitational alternative for dark energy. Phys ics Letters B 631 (1-2), pp. 1–6. Cited by: §I.

13. ∧T. Harko, F. S. Lobo, S. Nojiri, and S. D. Odintsov (2011) F (r, t) gravity. *Physical Review D—Particles, Fields, Gravitation, and Cosmology* 84 (2), pp. 024020. Cited by: §I.

14. ∧K. Bamba, S. D. Odintsov, L. Sebastiani, and S. Zerbini (2010) Finite-time future singularities in modified gauss−bonnet and 𝓕 (r, g) gravity and singularity avoidance. *The European Physical Journal C* 67, pp. 295−310. Cited by: §I.

15. ∧A. De la Cruz-Dombriz and D. Sáez-Gómez (2012) On the stability of the cosmological solutions in f (r, g) gravity. *Classical and Quantum Gravity* 29 (24), pp. 245014. Cited by: §I.

16. ∧J. B. Jiménez, L. Heisenberg, and T. Koivisto (2018) Coincident general relativity. *Physical Review D* 98 (4), pp. 044048. Cited by: §I.

17. ∧Y. Xu, G. Li, T. Harko, and S. Liang (2019) F (q, t) gravity. *The European Physical Journal C* 79, pp. 1−19. Cited by: §I.

18. ∧S. Bahamonde, K. F. Dialektopoulos, C. Escamilla-Rivera, G. Farrugia, V. Gakis, M. Hendry, M. Hohmann, J. L. Said, J. Mifsud, and E. Di Valentino (2023) Teleparallel gravity: from theory to cosmology. *Reports on Progress in Physics* 86 (2), pp. 026901. Cited by: §I.

19. a, bA. De, T. Loo, and E. N. Saridakis (2023) Non-metricity with bounday terms: f{(Q, C)} gravity and cosmology. *arXiv preprint arXiv:2308.00652*. Cited by: §I.

20. a, bS. Capozziello, V. De Falco, and C. Ferrara (2023) The role of the boundary term in f (q, b) symmetric teleparallel gravity. *The European Physical Journal C* 83 (10), pp. 915. Cited by: §I.

21. ∧G. N. Gadbail, A. De, and P. Sahoo (2023) Cosmological reconstruction and λ cdm universe in f (q, c) gravity. *The European Physical Journal C* 83 (12), pp. 1099. Cited by: §I.

22. a, bA. Samaddar, S. S. Singh, S. Muhammad, and E. E. Zotos (2024) Behaviours of rip cosmological models in f (q, c) gravity. *Nuclear Physics B* 1006, pp. 116643. External Links: ISSN 0550-3213 Cited by: §I, §III.

23. a, bD. C. Maurya (2024) Quintessence behaviour dark energy models in f (q, b)-gravity theory with observational constraints. *Astronomy and Computing* 46, pp. 100798. Cited by: §I, §III.

24. ∧D. C. Maurya (2024) Modified f (q, c) gravity dark energy models with observational constraints. *Modern Physics Letters A* 39 (10), pp. 2450034. Cited by: §I.

25. ∧D. Chandra Maurya (2024) Transit cosmological models in non-coincident gauge formulation of gravity theory with observational constraints. *Gravitation and Cosmology* 30 (3), pp. 330−343. Cited by: §I.

26. ∧D. C. Maurya (2024) Cosmology in non-coincident gauge formulation of f (q, c) gravity theory. *International Journal of Geometric Methods in Modern Physics* 21 (12), pp. 2450210−408. Cited by: §I.

27. ∧M. S. Turner and A. G. Riess (2002) Do type ia supernovae provide direct evidence for past deceleration of the universe?. *The Astrophysical Journal* 569 (1), pp. 18. Cited by: §I.

28. ∧A. G. Riess, L. Strolger, J. Tonry, S. Casertano, H. C. Ferguson, B. Mobasher, P. Challis, A. V. Filippenko, S. Jha, W. Li, et al. (2004) Type ia supernova discoveries at z¿ 1 from the hubble space telescope: evidence for past deceleration and constraints on dark energy evolution. *The Astrophysical Journal* 607 (2), pp. 665. Cited by: §I.

29. ^Y. Gong and A. Wang (2006) *Observational constraints on the acceleration of the universe. Physical Review D—Particles, Fields, Gravitation, and Cosmology* 73 (8), pp. 083506. Cited by: §I.

30. ^Y. Gong and A. Wang (2007) *Reconstruction of the deceleration parameter and the equation of state of dark energy. Physical Review D—Particles, Fields, Gravitation, and Cosmology* 75 (4), pp. 043520. Cited by: §I.

31. ^R. Nair, S. Jhingan, and D. Jain (2012) *Cosmokinetics: a joint analysis of standard candles, rulers and cosmic clocks. Journal of Cosmology and Astroparticle Physics* 2012 (01), pp. 018. Cited by: §I.

32. ^L. Xu and H. Liu (2008) *Constraints to deceleration parameters by recent cosmic observations. Modern Physics Letters A* 23 (23), pp. 1939–1948. Cited by: §I.

33. ^A. Shafieloo (2007) *Model-independent reconstruction of the expansion history of the universe and the properties of dark energy. Monthly Notices of the Royal Astronomical Society* 380 (4), pp. 1573–1580. Cited by: §I.

34. ^T. Holsclaw, U. Alam, B. Sansó, H. Lee, K. Heitmann, S. Habib, and D. Higdon (2011) *Nonparametric reconstruction of the dark energy equation of state from diverse data sets. Physical Review D—Particles, Fields, Gravitation, and Cosmology* 84 (8), pp. 083501. Cited by: §I.

35. ^T. Holsclaw, U. Alam, B. Sansó, H. Lee, K. Heitmann, S. Habib, and D. Higdon (2011) *Nonparametric reconstruction of the dark energy equation of state from diverse data sets. Physical Review D—Particles, Fields, Gravitation, and Cosmology* 84 (8), pp. 083501. Cited by: §I.

36. ^R. G. Crittenden, G. Zhao, L. Pogosian, L. Samushia, and X. Zhang (2012) *Fables of reconstruction: controlling bias in the dark energy equation of state. Journal of Cosmology and Astroparticle Physics* 2012 (02), pp. 048. Cited by: §I.

37. ^R. Nair, S. Jhingan, and D. Jain (2014) *Exploring scalar field dynamics with gaussian processes. Journal of Cosmology and Astroparticle Physics* 2014 (01), pp. 005. Cited by: §I.

38. ^T. Boehm and R. Brandenberger (2003) *On t-duality in brane gas cosmology. Journal of Cosmology and Astroparticle Physics* 2003 (06), pp. 008. Cited by: §I.

39. ^T. Padmanabhan (2003) *Cosmological constant—the weight of the vacuum. Physics reports* 380 (5-6), pp. 235–320. Cited by: §I.

40. ^Y. Gong and A. Wang (2007) *Reconstruction of the deceleration parameter and the equation of state of dark energy. Physical Review D—Particles, Fields, Gravitation, and Cosmology* 75 (4), pp. 043520. Cited by: §I.

41. ^a, ^b, ^c J. Cunha and J. A. S. d. Lima (2008) *Transition redshift: new kinematic constraints from supernovae. Monthly Notices of the Royal Astronomical Society* 390 (1), pp. 210–217. Cited by: §I, §III.

42. ^J. V. Cunha (2009) *Kinematic constraints to the transition redshift from supernovae type ia union data. Physical Review D—Particles, Fields, Gravitation, and Cosmology* 79 (4), pp. 047301. Cited by: §I.

43. ^B. Santos, J. C. Carvalho, and J. S. Alcaniz (2011) *Current constraints on the epoch of cosmic acceleration. Astroparticle Physics* 35 (1), pp. 17–20. Cited by: §I.

44. ^R. Nair, S. Jhingan, and D. Jain (2012) *Cosmokinetics: a joint analysis of standard candles, rulers and cosmic clocks. Journal of Cosmology and Astroparticle Physics* 2012 (01), pp. 018. Cited by: §I.

45. ∧ *A. Aviles, A. Bravetti, S. Capozziello, and O. Luongo (2013) Cosmographic reconstruction of f (t) cosmology. Physical Review D—Particles, Fields, Gravitation, and Cosmology 87 (6), pp. 064025. Cited by: §I.*

46. a, b *A. Samaddar and S. S. Singh (2024) Constraining model parameters in f (q, c) gravity: observational analysis and geometric diagnostics. arXiv preprint arXiv:2411.17754. Cited by: §II, §VI.*

47. ∧ *A. De, T. Loo, and E. N. Saridakis (2024) Non-metricity with boundary terms: (,) gravity and cosmology. Journal of Cosmology and Astroparticle Physics 2024 (03), pp. 050. Cited by: §II.*

48. ∧ *N. Banerjee and S. Das (2005) Acceleration of the universe with a simple trigonometric potential. General Relativity and Gravitation 37, pp. 1695–1703. Cited by: §III.*

49. ∧ *C. Escamilla-Rivera and A. Nájera (2022) Dynamical dark energy models in the light of gravitational-wave transient catalogues. Journal of Cosmology and Astroparticle Physics 2022 (03), pp. 060. Cited by: §III.*

50. ∧ *M. S. Turner and A. G. Riess (2002) Do type ia supernovae provide direct evidence for past deceleration of the universe?. The Astrophysical Journal 569 (1), pp. 18. Cited by: §III.*

51. ∧ *A. G. Riess, L. Strolger, J. Tonry, S. Casertano, H. C. Ferguson, B. Mobasher, P. Challis, A. V. Filippenko, S. Jha, W. Li, et al. (2004) Type ia supernova discoveries at z¿ 1 from the hubble space telescope: evidence for past deceleration and constraints on dark energy evolution. The Astrophysical Journal 607 (2), pp. 665. Cited by: §III.*

52. ∧ *Y. Gong and A. Wang (2006) Observational constraints on the acceleration of the universe. Physical Review D—Particles, Fields, Gravitation, and Cosmology 73 (8), pp. 083506. Cited by: §III.*

53. ∧ *L. Xu and H. Liu (2008) Constraints to deceleration parameters by recent cosmic observations. Modern Physics Letters A 23 (23), pp. 1939–1948. Cited by: §III.*

54. ∧ *S. Del Campo, I. Duran, R. Herrera, and D. Pavon (2012) Three thermodynamically based parametrizations of the deceleration parameter. Physical Review D—Particles, Fields, Gravitation, and Cosmology 86 (8), pp. 083509. Cited by: §III.*

55. ∧ *A. Al Mamon and S. Das (2016) A divergence-free parametrization of deceleration parameter for scalar field dark energy. International Journal of Modern Physics D 25 (03), pp. 1650032. Cited by: §III.*

56. ∧ *D. S. Rana, R. Solanki, and P. Sahoo (2024) Phase-space analysis of the viscous fluid cosmological models in the coincident f (q) gravity. Physics of the Dark Universe 43, pp. 101421. Cited by: §III.*

57. ∧ *M. P. Hobson ((2010)) Bayesian methods in cosmology. Cambridge University Press. Cited by: §IV.*

58. ∧ *H. Singirikonda and S. Desai ((2020)) Model comparison of λ cdm vs r h= ct using cosmic chronometers. The European Physical Journal C 80 (8), pp. 694. Cited by: §IV.1.*

59. ∧ *M. Kowalski, D. Rubin, G. Aldering, R. Agostinho, A. Amadon, R. Amanullah, C. Balland, K. Barbary, G. Blanc, P. J. Challis, et al. ((2008)) Improved cosmological constraints from new, old, and combined supernova data sets. The Astrophysical Journal 686 (2), pp. 749. Cited by: §IV.2.*

60. ∧ *R. Amanullah, C. Lidman, D. Rubin, G. Aldering, P. Astier, K. Barbary, M. Burns, A. Conley, K. Dawson, S. Deustua, et al. ((2010)) Spectra and hubble space telescope light curves of six type ia supernovae at 0.511¡ z¡ 1.12 and the union2*

compilation. The Astrophysical Journal 716 (1), pp. 712. Cited by: §IV.2.

61. ∧*N. Suzuki, D. Rubin, C. Lidman, G. Aldering, R. Amanullah, K. Barbary, L. Barrientos, J. Botyanszki, M. Brodwin, N. Connolly, et al. ((2012)) The hubble space telescope cluster supernova survey. v. improving the dark-energy constraints above z¿ 1 and building an early-type-hosted supernova sample. The Astrophysical Journal 746 (1), pp. 85. Cited by: §IV.2.*

62. ∧*M. Betoule, R. Kessler, J. Guy, J. Mosher, D. Hardin, R. Biswas, P. Astier, P. El-Hage, M. Konig, S. Kuhlmann, et al. ((2014)) Improved cosmological constraints from a joint analysis of the sdss-ii and snls supernova samples. Astronomy & Astrophysics 568, pp. A22. Cited by: §IV.2.*

63. ∧*D. M. Scolnic, D. Jones, A. Rest, Y. Pan, R. Chornock, R. Foley, M. Huber, R. Kessler, G. Narayan, A. Riess, et al. ((2018)) The complete light-curve sample of spectroscopically confirmed sne ia from pan-starrs1 and cosmological constraints from the combined pantheon sample. The Astrophysical Journal 859 (2), pp. 101. Cited by: §IV.2.*

64. ∧*D. Scolnic, D. Brout, A. Carr, A. G. Riess, T. M. Davis, A. Dwomoh, D. O. Jones, N. Ali, P. Charvu, R. Chen, et al. (2022) The pantheon+ analysis: the full data set and light-curve release. The Astrophysical Journal 938 (2), pp. 113. Cited by: §IV.2.*

65. ∧*V. Sahni, T. D. Saini, A. A. Starobinsky, and U. Alam (2003) Statefinder—a new geometrical diagnostic of dark energy. Journal of Experimental and Theoretical Physics Letters 77, pp. 201–206. Cited by: §V.4.*

66. ∧*C. Zunckel and C. Clarkson (2008) Consistency tests for the cosmological constant. Physical review letters 101 (18), pp. 181301. Cited by: §V.5.*

67. ∧*V. Sahni, A. Shafieloo, and A. A. Starobinsky (2008) Two new diagnostics of dark energy. Physical Review D—Particles, Fields, Gravitation, and Cosmology 78 (10), pp. 103502. Cited by: §V.5.*

68. ∧*S. Bhoyar and Y. B. Ingole (2024) Resolving flrw cosmology through effective equation of state in f (t) gravity. Chinese Journal of Physics 92, pp. 1085–1096. Cited by: §VI.*

69. ª, ᵇ*G. N. Gadbail, S. Mandal, and P. K. Sahoo (2022) Parametrization of deceleration parameter in f (q) gravity. Physics 4 (4), pp. 1403–1412. Cited by: §VI, §VI.*

70. ∧*A. A. Mamon and S. Das (2017) A parametric reconstruction of the deceleration parameter. The European Physical Journal C 77 (7), pp. 495. Cited by: §VI.*

71. ∧*R. Solanki, A. De, S. Mandal, and P. Sahoo (2022) Accelerating expansion of the universe in modified symmetric teleparallel gravity. Physics of the Dark Universe 36, pp. 101053. Cited by: §VI.*

72. ∧*V. K. Bhardwaj and A. Pradhan (2022) Evaluation of cosmological models in f (r, t) gravity in different dark energy scenario. New Astronomy 91, pp. 101675. Cited by: §VI.*

73. ∧*P. S. Singh and K. P. Singh (2021) F (r, t) gravity model behaving as a dark energy source. New Astronomy 84, pp. 101542. Cited by: §VI.*

74. ∧*A. Dixit, V. K. Bhardwaj, and A. Pradhan (2020) RHDE models in frw universe with two ir cut-offs with redshift parametrization. The European Physical Journal Plus 135 (10), pp. 1–13. Cited by: §VI.*

75. ^ S. Ghaffari (2022) *Kaniadakis holographic dark energy in brans–dicke cosmology. Modern Physics Letters A 37 (2 3), pp. 2250152. Cited by: §VI.*

76. a, b S. Bhoyar, Y. B. Ingole, and A. Kale (2024) *Generalized ghost pilgrim dark energy fractal cosmology with observational constraint. Physica Scripta 100 (1), pp. 015026. Cited by: §VI, §VI.*

77. ^ S. Bhoyar and Y. B. Ingole (2024) *Cosmic evolution of the kantowski-sachs universe in the context of a bulk viscous string in teleparallel gravity. Indian Journal of Physics, pp. 1–13. Cited by: §VI.*

78. ^ G. N. Gadbail, S. Arora, and P. Sahoo (2022) *Generalized chaplygin gas and accelerating universe in f (q, t) gravity. Physics of the Dark Universe 37, pp. 101074. Cited by: §VI.*

79. ^ A. Al Mamon, V. C. Dubey, and K. Bamba (2021) *Statefinder and om diagnostics for new generalized chaplygin gas model. Universe 7 (10), pp. 362. Cited by: §VI.*

80. ^ V. Gorini, A. Kamenshchik, and U. Moschella (2003) *Can the chaplygin gas be a plausible model for dark energy?. Physical Review D 67 (6), pp. 063509. Cited by: §VI.*

81. ^ G. N. Gadbail, S. Arora, and P. Sahoo (2021) *Viscous cosmology in the weyl-type f (q, t) gravity. The European Physical Journal C 81 (12), pp. 1088. Cited by: §VI.*

82. ^ A. Pradhan, A. Dixit, and V. K. Bhardwaj (2021) *Barrow hde model for statefinder diagnostic in flrw universe. International Journal of Modern Physics A 36 (04), pp. 2150030. Cited by: §VI.*

Declarations